Lattice QED in external electromagnetic fields

D. K. Sinclair and J. B. Kogut

- Introduction
- Lattice QED in an external Magnetic Field
- Simulations and results
- Difficulties to be overcome to extend this to include the Electric Field
- Discussions and Conclusions

Introduction

QED in external electromagnetic fields has applications in Laser Physics, Accelerator physics, Astrophysics and Condensed Matter physics.

While electrons in external Electric Fields exhibit some of the more interesting phenomena (from our perspective) such as the Sauter-Schwinger effect – electron-positron production in (strong) electric fields – the introduction of external electric fields leads to a complex action making standard simulation techniques inapplicable.

Hence for our first project we will consider QED in external magnetic fields, where the action remains real.

Classically charged particles in a magnetic field have helical trajectories around magnetic field lines. This means that while the motion in the direction of the magnetic field is free, that in the plane transverse to the magnetic field is bound.

Quantum mechanics forces the motion in this transverse plane

to be quantized into a set of discrete transverse energy levels – the Landau levels.

Increasing the magnetic field decreases the transverse spread of such orbits and increases the energy gap between these levels until eventually all electrons will occupy the lowest level. This leads to the dimensional reduction from 3+1 to 1+1.

We simulate lattice QED in a constant external magnetic field using the RHMC method developed for lattice QCD. Since QED does not have an ultra-violet completion, we consider it as an effective field theory.

While the only chiral symmetry in QED is broken by the anomaly, (finite order) perturbative QED exhibits some of the properties of a theory with an unbroken chiral symmetry. In the limit of zero bare mass, the renormalized mass also approaches zero. Similarly, $\langle \bar{\psi}\psi \rangle \to 0$ in this limit.

Free electrons in a constant external magnetic field B also remain massless in the limit of zero bare mass, and again $\langle\bar{\psi}\psi\rangle \to 0$. However, there is an extra term $m|eB| \ln\left(\frac{|eB|}{m^2}\right)$ in this approach, which is clearly non-perturbative.

When the effects of QED are included, approximate methods (Schwinger-Dyson, Bethe-Salpeter,...) indicate that the electron develops a dynamical mass

$$m_{\rm dynamical} \sim \sqrt{|eB|}\exp\left(-\frac{\pi}{2}\sqrt{\frac{\pi}{2\alpha}}\right)$$

which is non-perturbative and should make a related contribution to $\langle\bar{\psi}\psi\rangle$, which will not vanish as $m \to 0$.

In our simulations we try to determine whether such a contribution to $\langle\bar{\psi}\psi\rangle$ exists. Because $m_{\rm dynamical}$ is predicted to be so small – $\sim 10^{-10} \times \sqrt{eB}$ – for $\alpha = 1/137$, we are also running at stronger coupling – $\alpha = 1/10$ – where $m_{\rm dynamical} \sim 10^{-3} \times \sqrt{eB}$ by the above, and multi-loop contributions are

expected to make this even larger.

So far our results are suggestive but inconclusive.

We are also storing configurations on which to measure the asymmetries and screenings of coulomb potentials, which are predicted to occur for QED in strong external magnetic fields. These should be large enough to be measurable in our simulations at a physical α value.

Lattice QED in an external Magnetic Field

We simulate using the non-compact gauge action

$$S(A) = \frac{\beta}{2}\sum_{n,\mu<\nu}[A_\nu(n+\hat{\mu}) - A_\nu(n) - A_\mu(n+\hat{\nu}) + A_\mu(n)]^2$$

where n is summed over the lattice sites and μ and ν run from 1 to 4 subject to the restriction. $\beta = 1/e^2$. The functional integral to calculate the expectation value for an observable $\mathcal{O}(\mathcal{A})$ is then

$$\langle \mathcal{O} \rangle = \frac{1}{Z}\int_{-\infty}^{\infty} \Pi_{n,\mu} dA_\mu(n) e^{-S(A)} [\det \mathcal{M}(A+A_{ext})]^{1/8} \mathcal{O}(\mathcal{A})$$

where $\mathcal{M} = M^\dagger M$ and M is the staggered fermion action in the presence of the dynamic photon field A and external photon field A_{ext} describing the magnetic field B (or rather eB). M is defined by

$$M(A + A_{ext}) = \sum_\mu D_\mu(A + A_{ext}) + m$$

where the operator D_μ is defined by

$$[D_\mu(A + A_{ext})\psi](n) = \frac{1}{2}\eta_\mu(n)\{e^{i(A_\mu(n)+A_{ext,\mu}(n))}\psi(n+\hat{\mu}) - e^{-i(A_\mu(n-\hat{\mu})+A_{ext,\mu}(n-\hat{\mu}))}\psi(n-\hat{\mu})\}$$

and η_μ are the staggered phases. Note that this treatment of the gauge-field–fermion interactions is compact and so has period 2π in the gauge fields.

We implement the RHMC simulation method of Clark and Kennedy, using a $(20, 20)$rational approximation to $\mathcal{M}^{-1/8}$ and $(12, 12)$ rational approximations $\mathcal{M}^{\pm 1/16}$. To account for the range of normal modes of the non-compact gauge action we vary the trajectory lengths τ over the range

$$\frac{\pi}{2\sqrt{\beta}} \leq \tau \leq \frac{4\pi}{\sqrt{2\beta(4 - \sum_\mu \cos(2\pi/N_\mu))}}$$

, of the periods of the modes of this gauge action.

A_{ext} are chosen in the symmetric gauge as

$$A_{ext,1}(i,j,k,l) = -\frac{eB}{2} \quad (j-1) \quad i \neq N_1$$

$$A_{ext,1}(i,j,k,l) = -\frac{eB}{2}(N_1+1) \quad (j-1) \quad i = N_1$$

$$A_{ext,2}(i,j,k,l) = +\frac{eB}{2} \quad (i-1) \quad j \neq N_2$$

$$A_{ext,2}(i,j,k,l) = +\frac{eB}{2}(N_2+1) \quad (i-1) \quad j = N_2$$

while $A_{ext,3}(n) = A_{ext,4}(n) = 0$. In practice we subtract the average values of A_{ext}, μ from these definitions. This choice produces a magnetic field eB in the $+z$ direction on every $1,2$ plaquette except that with $i = N_1$, $j = N_2$, which has the magnetic field $eB(1 - N_1N_2)$. Because of the compact nature of the interaction, requiring $eBN_1N_2 = 2\pi n$ for some integer $n = 0, 1, ...N_1N_2/2$ makes the value of this plaquette indistinguishable from eB. Hence $eB = 2\pi n/(N_1N_2)$ lies in the interval

$[0, \pi]$.

One of the observables we calculate is the electron contribution to the effective gauge action per site $\frac{-1}{8V}\mathbf{trace}[\mathbf{ln}(\mathcal{M})]$. For $\mathbf{ln}(\mathcal{M})$ we use a $(30, 30)$ rational approximation to the logarithm. Here we use the Chebyshev method of Kelisky and Rivlin. While this has worse errors than a Remez approach, it preserves some of the properties of the logarithm itself, and is applicable on the whole complex plane cut along the negative real axis.

Simulations and results

We are simulating QED (1-flavour) on a 36^4 lattice with electron mass $m = 0.1$ and $m = 0.2$ in an external magnetic field B. Most of our simulations are performed at $\alpha = 1/137$. Note that with these choices the momentum cutoff is so low that the difference between the bare(lattice) coupling and mass and the renormalized coupling and mass are at most a few percent, and are neglected.

We test the range of applicability of the lattice approach by first calculating

$$\langle\bar{\psi}\psi\rangle = \frac{1}{4V}\mathbf{trace}[M^{-1}(A_{ext})]$$

as a function of allowed eB values on the lattice, and comparing it to the known continuum result:

$$\langle\bar{\psi}\psi\rangle = \langle\bar{\psi}\psi\rangle|_{eB=0} + \frac{meB}{4\pi^2}\int_0^\infty \frac{ds}{s} e^{-sm^2}\left[\coth(eBs) - \frac{1}{eBs}\right].$$

Next we calculate

$$\begin{aligned}\mathcal{L}_f &= -\frac{1}{4V}\ln\{\det[M(A_{ext})]\} \\ &= -\frac{1}{4V}\mathrm{trace}\{\ln[M(A_{ext})]\}\end{aligned}$$

on the lattice, and compare it with the known continuum result:

$$\begin{aligned}\mathcal{L}_f = \mathcal{L}_f|_{B=0} &+ \frac{(eB)^2}{24\pi^2}\int_0^\infty \frac{ds}{s}e^{-m^2 s} \\ &+ \frac{eB}{8\pi^2}\int_0^\infty \frac{ds}{s^2}e^{-m^2 s}\left[\coth(eBs) - \frac{1}{eBs} - \frac{eBs}{3}\right].\end{aligned}$$

In both cases we take the lattice values for the divergent parts of these observables in their continuum versions.

Figure 1 shows the comparison between the lattice and continuum values for $\langle\bar{\psi}\psi\rangle$ for free electrons in a constant external magnetic field B for electron masses $m = 0.1$ and $m = 0.2$. Note that the agreement between lattice and continuum results is reasonable for $eB \lesssim 0.63$ or $\pi/5$. The agreement is better for

larger lattices, but the range of Bs where the agreement is good is no better.

Figure 2 compares the lattice and continuum values of the fermion contribution to the effective action from free electrons in a constant external magnetic field $\mathcal{L}_f$ for electron masses $m = 0.1$ and $m = 0.2$. Again there is reasonable agreement between lattice and continuum results over a limited range of B values.

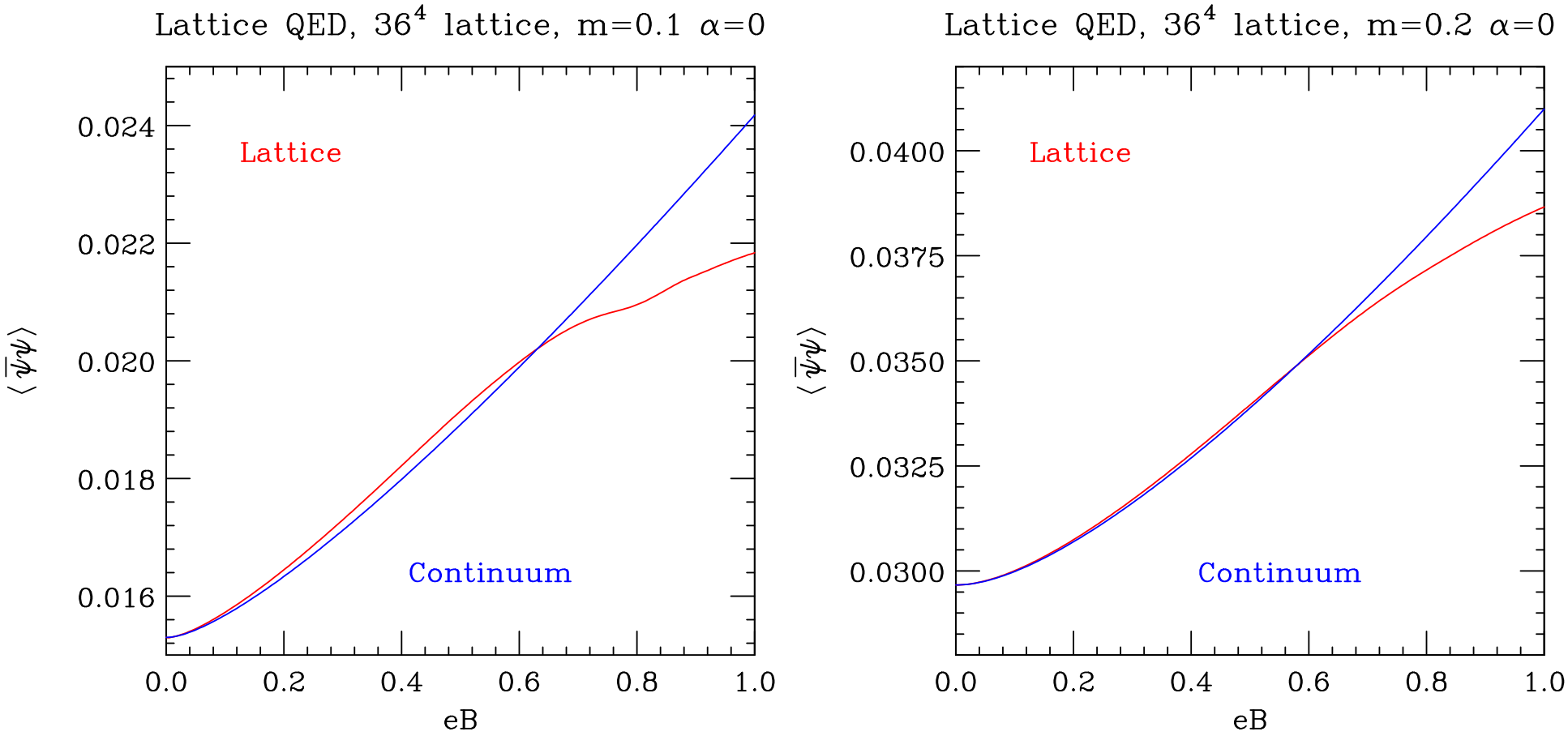

Figure 1: Free-electron $\langle\bar{\psi}\psi\rangle$ as functions of eB, comparing the continuum and lattice results for a) $m = 0.1$ and b) $m = 0.2$.

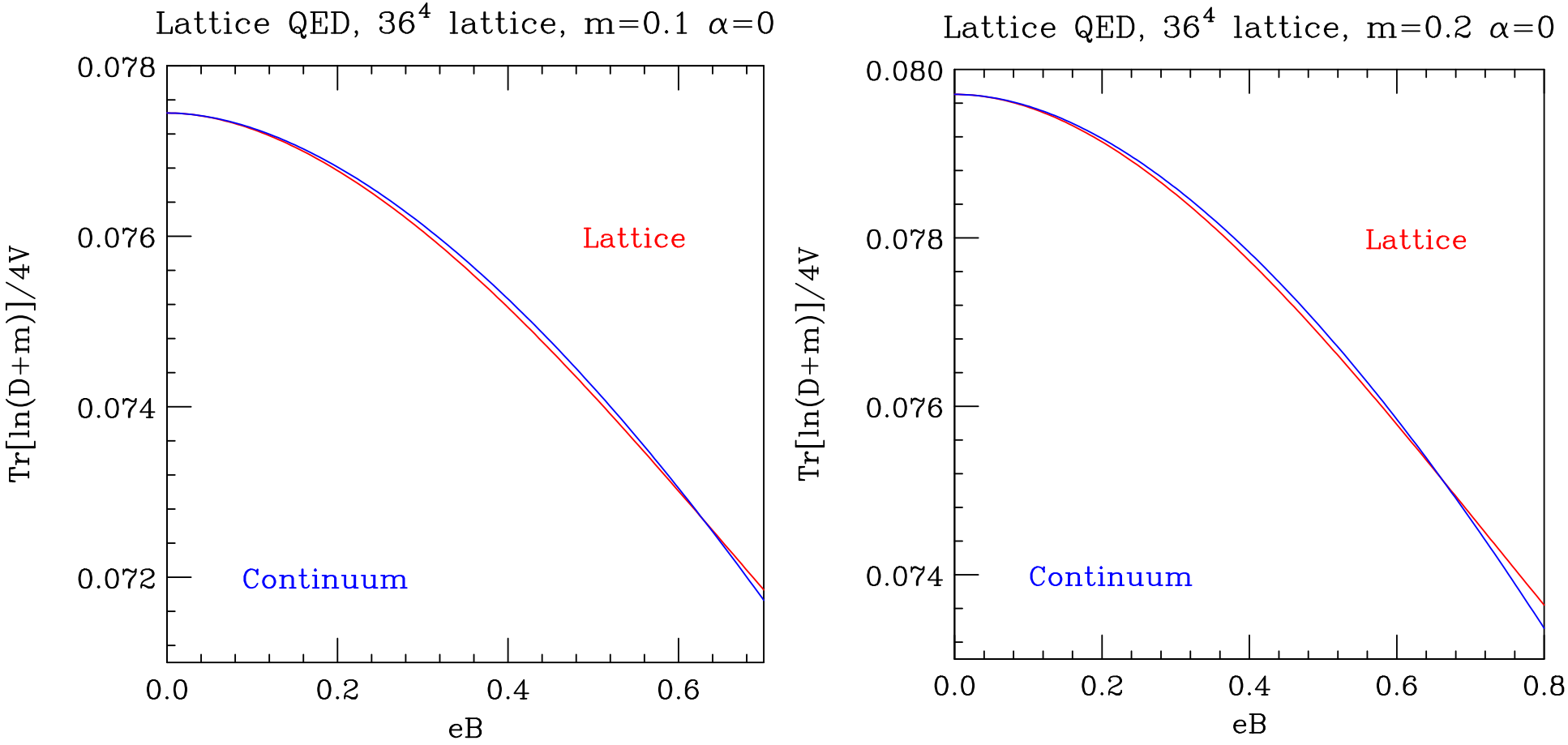

Figure 2: Free-field $-\mathcal{L}_f$ as functions of eB, comparing the continuum and lattice results for a) $m = 0.1$ and b) $m = 0.2$.

We simulate QED with one electron in a (strong) constant magnetic field on a $\mathbf{36}^4$ lattice with periodic boundary conditions at $\boldsymbol{\alpha = 1/137}$ for a range of (allowed) values of $\boldsymbol{eB}$ from $\mathbf{0}$ to $\boldsymbol{eB}$ sufficiently large that discretization errors become appreciable, at electron masses $\boldsymbol{m = 0.1}$ and $\boldsymbol{m = 0.2}$. At each $\boldsymbol{eB}$ and $\boldsymbol{m}$, we run for 12500 trajectories, storing a gauge configuration every 100 trajectories for further analysis.

Figure 3 shows $\langle\bar{\psi}\psi\rangle$ from these runs, which demonstrates that the main effect of QED is to increase the magnitudes of $\langle\bar{\psi}\psi\rangle$. Following the trend of the free field values, it increases as $\boldsymbol{eB}$ increases.

Figure 4 shows the effective action $\boldsymbol{\mathcal{L}_f}$ from these runs. Here QED reduces the magnitude of the effective action whose $\boldsymbol{eB}$ dependence is similar to that of the free field case, i.e. it decreases as $\boldsymbol{eB}$ increases.

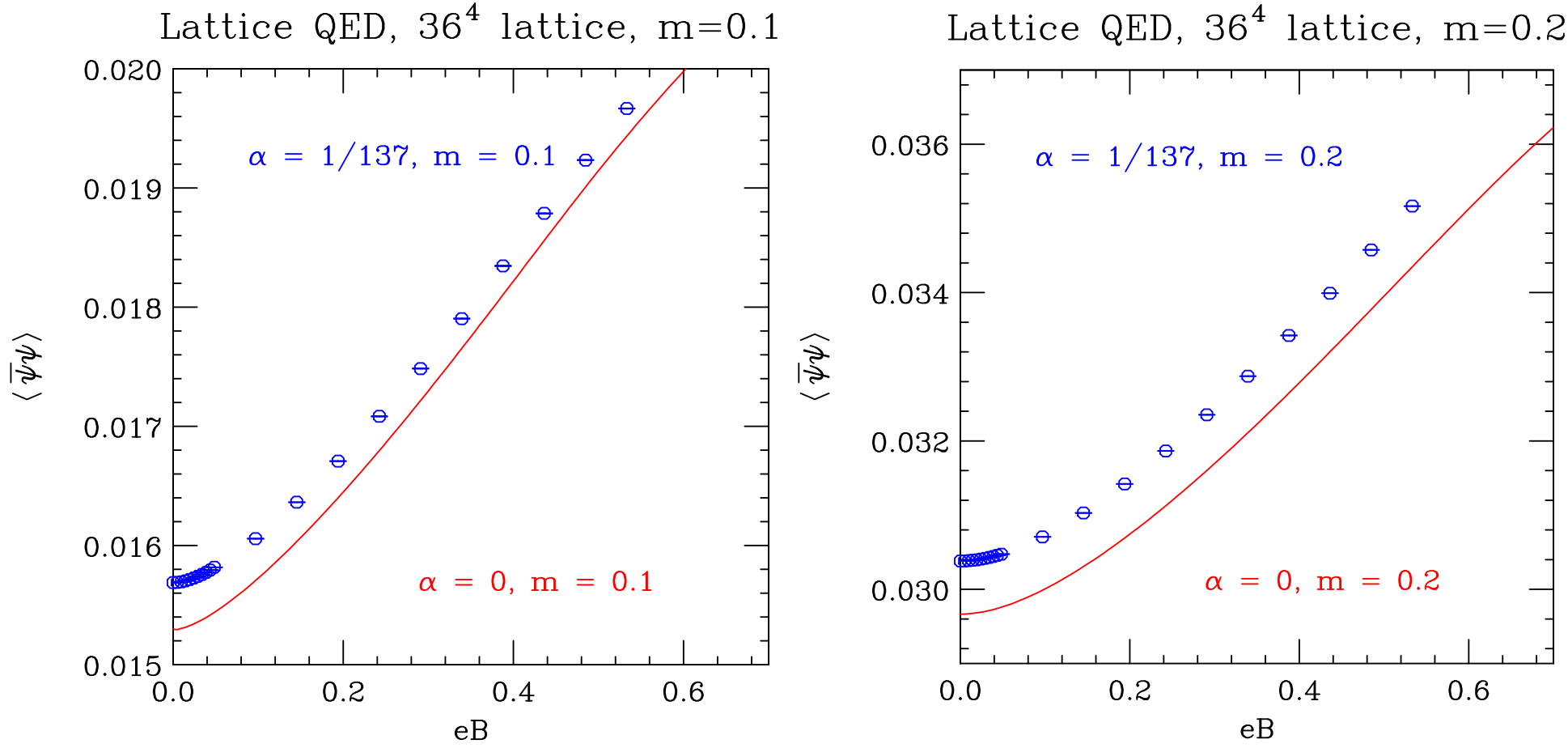

Figure 3: Electron $\langle\bar{\psi}\psi\rangle$ as functions of eB, comparing the continuum and lattice results for a) $m = 0.1$ and b) $m = 0.2$.

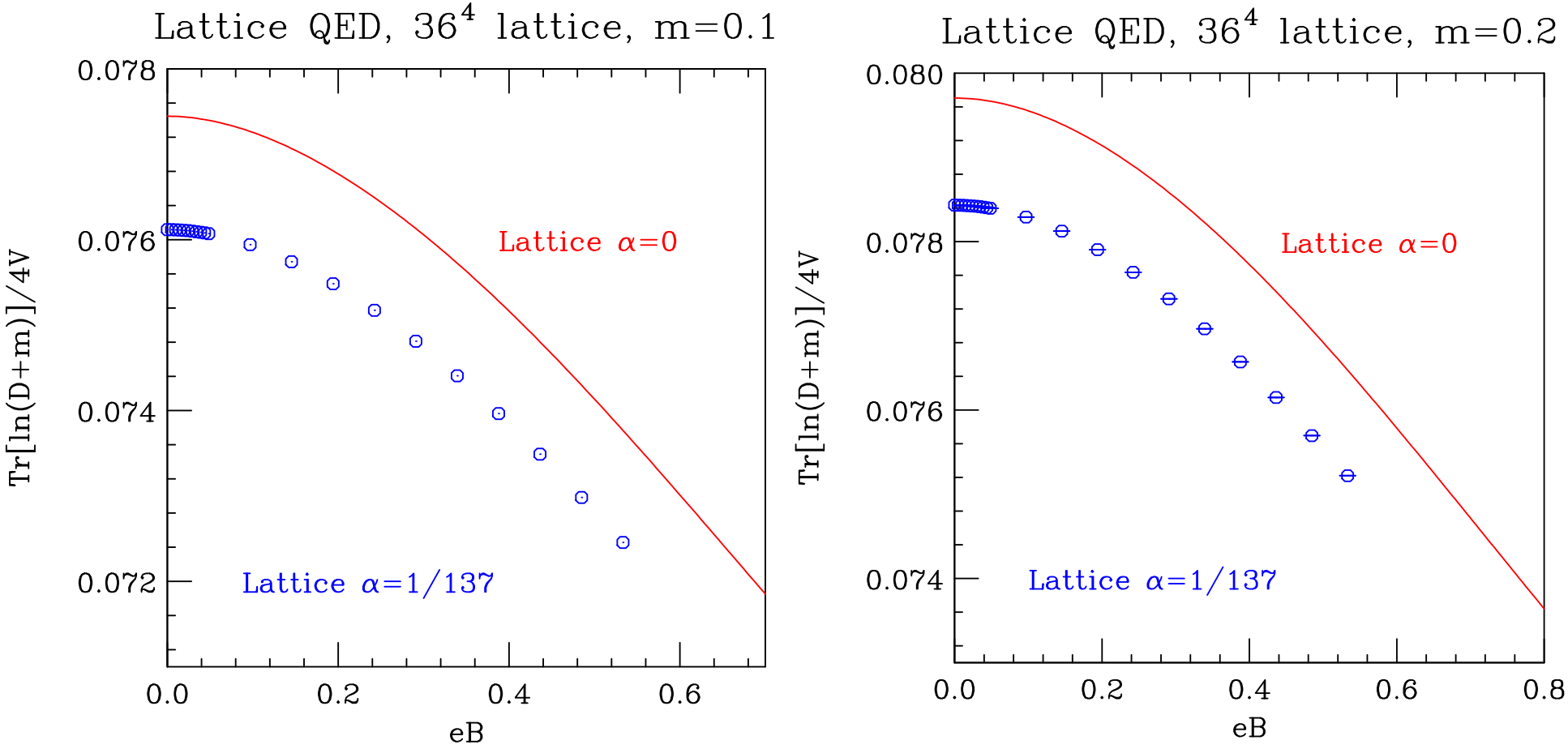

Figure 4: $-\mathcal{L}_f$ as functions of eB, comparing the free field ($\alpha = 0$) and QED ($\alpha = 1/137$) results for a) $m = 0.1$ and b) $m = 0.2$.

We are interested to know if the electron develops a dynamical mass. If so this should feed back into $\langle\bar{\psi}\psi\rangle$, which should no longer vanish in the $m \to 0$ limit. However, since it has been estimated that for $\alpha = 1/137$, $eB \sim 1$ the dynamical electron mass will be $\sim 10^{-10}$, which is unobservable, we have performed simulations at $\alpha = 1/10$ where the dynamical electron mass is estimated to be $\sim 10^{-3}$ for $eB \sim 1$ and could well be larger since this is in the regime where multiloop diagrams are at least as important as 1-loop diagrams. We are planning simulations at $\alpha = 1$ where the maximum dynamical mass should be ~ 0.1.

Figure 5 shows $\langle\bar{\psi}\psi\rangle$ at $m = 0.2$, $m = 0.1$, and a linear extrapolation to $m = 0$, for $\alpha = 0$, $\alpha = 1/137$, and $\alpha = 1/10$. The 3 eB values for the lower 2 αs are 0, $(2\pi/36^2) \times 50 = 0.2424...$ and $(2\pi/36^2) \times 100 = 0.4848...$. For the highest α, the 2 eB values are 0 and $(2\pi/36^2) \times 100 = 0.4848...$.

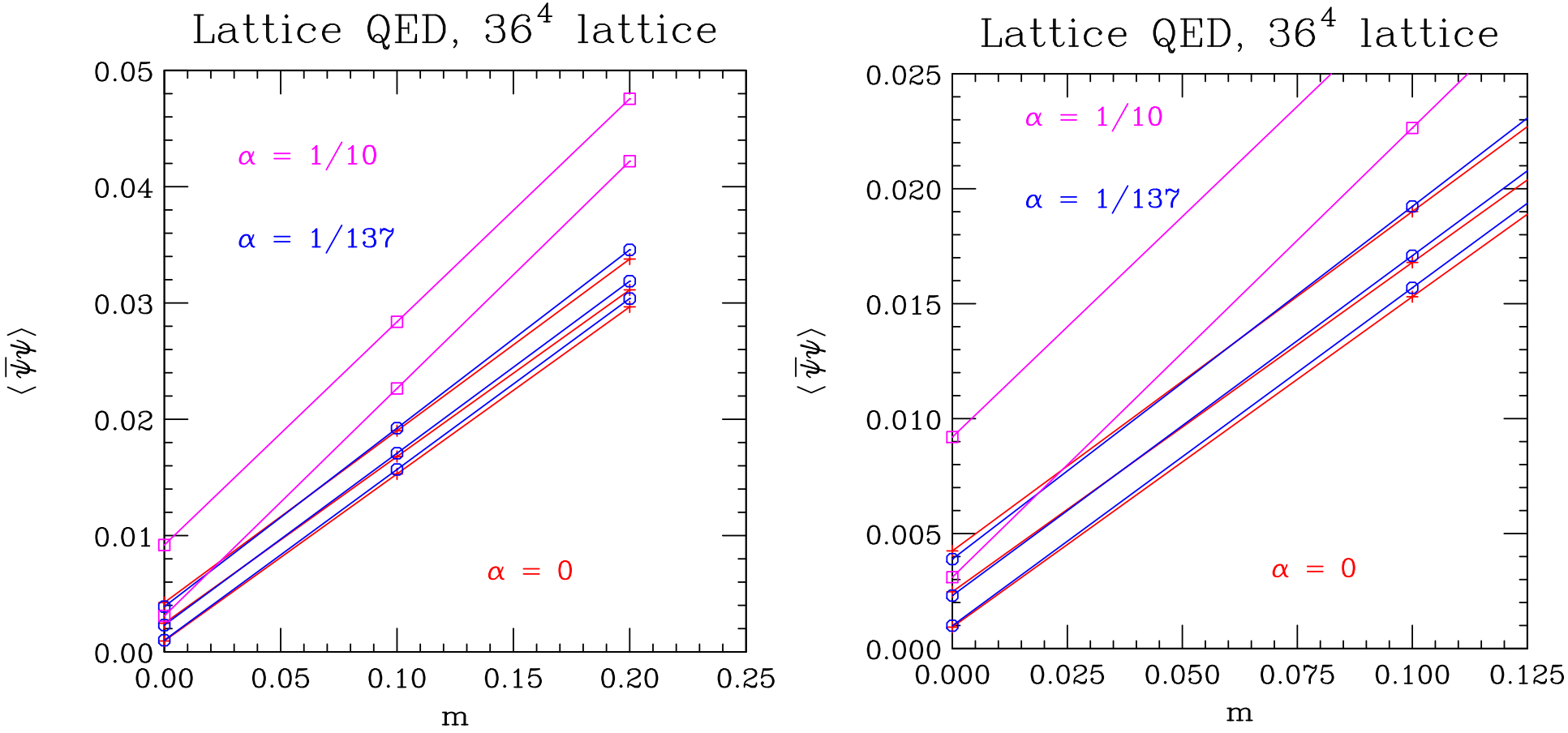

Figure 5: $\langle \bar{\psi}\psi \rangle$ as functions of mass for $\alpha = 0$, $\alpha = 1/137$, and $\alpha = 1/10$, and various eBs.

We know that for $\alpha = 0$, $\langle \bar{\psi}\psi \rangle$ vanishes in the $m = 0$ limit. For $\alpha = 1/137$, the linear extrapolation gives results similar to those at $\alpha = 0$, indicating that $\langle \bar{\psi}\psi \rangle$ either vanishes or becomes very small in this limit. For $\alpha = 1/10$ the situation is less clear, and it will need smaller mass simulations to determine the curvature of these fits. Larger α will help.

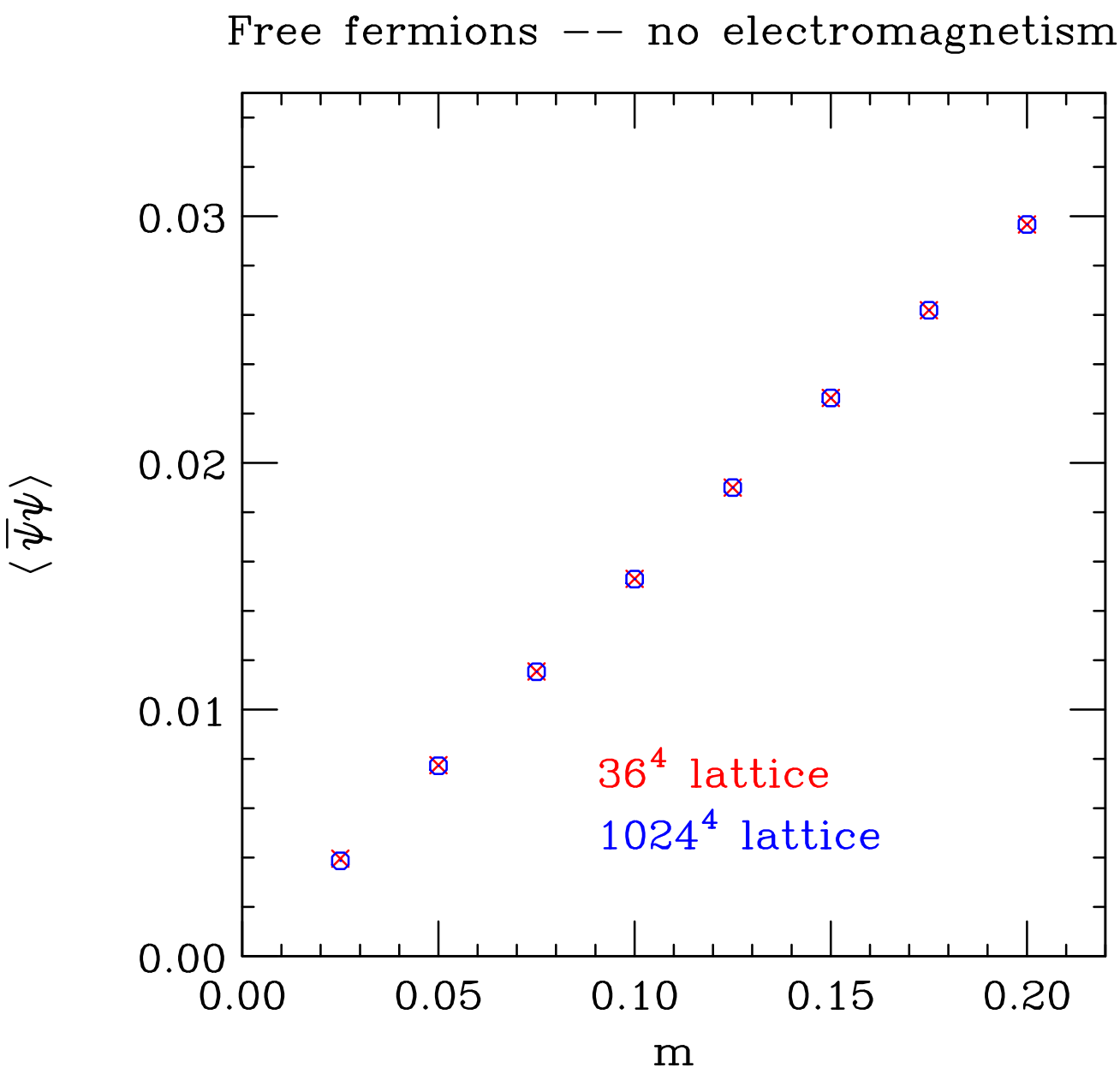

Figure 6: $\langle \bar{\psi}\psi \rangle$ as a function of mass m for free electrons and no magnetic field. Note how small the finite lattice size effects are.

Difficulties to be overcome to extend this to include the Electric Field

Contour rotation to imaginary time and imaginary A_4 leaves $A_{ext,4}$ real. Hence the euclidean action is complex, so traditional simulation methods cannot be applied.

For QED, the pure gauge action is just a collection of harmonic oscillators, so if one applies complex-langevin simulations, the real trajectory is attractive, unlike in QCD where the real trajectory is repulsive. It remains to be seen if this property survives the addition of real fermion dynamics (QED without external electric fields.

Can one analytically continue from imaginary $A_{ext,4}$ with its real euclidean action to real $A_{ext,4}$ with its complex action?

The rational approximation we use for $\ln$ does work for complex arguments. Can multimass inversions be performed as for positive definite matrices, or will we need to perform 30 separate inversions?

Because the exponential interactions of the gauge fields with

fermions are now exponentials of real numbers, one cannot use periodicity to simplify periodic boundary conditions. What is the best way to implement boundary conditions?

Discussions and conclusions

- We simulate lattice QED in a constant background magnetic field at close to the physical value of $\alpha = \frac{e^2}{4\pi}$ at $m = 0.1$ and $m = 0.2$ in lattice units. These simulations should enable us to access some of the effects due to Landau levels, which result in an effective dimensional reduction from $3+1$ dimensions to $1+1$ dimensions, with various non-perturbative consequences.
- $\langle \bar{\psi}\psi \rangle$ is measured as a function of B to test whether it vanishes in the $m \to 0$ limit. Comparing it with the behaviour for free electrons at the same values of the magnetic field, we conclude that we see no evidence of a non-zero limit, which would be evidence for the production of a dynamical electron mass proportional to $\sqrt{eB}$.
- However, the predicted value for such a non-perturbative mass is far too small to be observed for the values of eB accessible to these simulations at the physical value of α. We therefore simulate at an unphysically large coupling $\alpha = 1/10$. However,

with only 2 masses we can only perform a linear extrapolation to $m = 0$ which does not allow us to account for curvature in this extrapolation.

- We are therefore starting simulations at an even larger coupling ($\alpha = 1$) where one can hope that the effect will be large. At this coupling, as well as at $\alpha = 1/10$ we hope to also simulate at an even smaller mass, to help with the extrapolation to m=0. However, this will require a larger lattice – 64^4 or 72^4 – which will be expensive.
- During our simulations we have stored 125 configurations for each value of m, eB and α. We will use these to examine the effects the magnetic field has on coulomb interactions between electron-positron pairs. These include breaking of the rotational symmetry and screening. These effects should be measurable even at physical α values.
- We will also measure the electron propagator on stored configurations. At large α, this should enable direct measurement

of any (non-perturbative) dynamical electron mass to check the predictions of calculations using approximations having less controllable systematic errors.

- We plan to perform simulations of QED in external Electric Fields, where the Sauter-Schwinger effect will manifest itself by the effective gauge action generated by the electron fields developing an imaginary part, heralding the production of electron-positron pairs from the vacuum.

These simulations were performed on the Bebop Cluster at ANL, Cori at NERSC using an ERCAP(DOE) allocation, and using XSEDE(NSF) allocations on Expanse at UCSD, Bridges-2 at PSC and Stampede-2 at TACC.

One of us (DKS) would like to thank G. T. Bodwin for helpful discussions, while JBK would like to acknowledge conversations with A. Shovkovy and V. Yakimenko.